JOURNAL OF AIRCRAFT
Vol. 31, No. 4, July–Aug. 1994

Parametric Studies of Bearing Strength for Fiber/Metal Laminates

H. Felix Wu*
Alcoa Technical Center, Alcoa Center, Pennsylvania 15069
and
Wim J. Slagter†
Delft University of Technology, Delft, The Netherlands

An experimental program based on statistical design was conducted to establish a meaningful test procedure for determination of fiber/metal laminate bearing strength design allowables. The test procedures investigated are the pin-type bearing test method (ASTM E-238) and the bolt-type bearing test method, a modified method based on procedure for bearing strength determinations in plastics (ASTM D-953). Results are presented from an experimental program which measured the bearing strengths of two grades of S-2 glass fiber-based and one grade of aramid fiber-based aluminum laminates. The influences of lateral constraint and ply orientation on bearing strength and failure mode are observed. The bolt-type bearing test method which combines the attributes of two aforementioned methods is recommended. The study also showed that bearing properties of edge distance ratio equals to 2 can be predicted by correlation with the aluminum volume fraction in fiber-reinforced aluminum laminates. In addition, diagrams of joint structural efficiency shown to be comparable with aluminum alloy sheets have been established.

I. Introduction

FIBER/METAL laminates are arrangements of thin, high-strength aluminum alloy sheets bonded to alternating plies of fiber-reinforced epoxy-adhesive. They represent a new class of aerospace sheet materials that combine the best features of pure composites and metals.[1–12] Fiber/metal laminates offer the same magnitude of weight reduction[13–15] and structural performance as graphite/epoxy composites while retaining the familiar design, manufacturability, and supportability characteristics of aluminum. Fiber/metal laminates provide the opportunity for distinctive advances in structures at a much lower risk than graphite/epoxy composites. In addition, fiber/metal laminates also exhibit good thermal stability in both cryogenic and elevated temperature environments.[16–18]

Presently, fiber/metal laminates are the only available structural sheet materials that combine the fatigue insensitivity of composites with the damage tolerant capability of metals. Their ability to impede and arrest crack growth makes them promising candidates as fuselage materials in next generation civil transport aircraft. Development of fiber/metal laminates to meet the stringent demands of fuselage applications could revolutionize airframe construction by providing aircraft designers with a robust portfolio of high-performance, engineered materials. The need for such materials is graphically demonstrated by current problems and safety concerns with our "aging aircraft" fleet.

First- and second-generation laminate forms given in Tables 1 and 2 have been standardized as product benchmarks. Each product benchmark employs thin, high-strength (7475- or 2024-type) aluminum alloy sheets alternated with layers of adhesive-impregnated fibers. A generic schematic representation of a 3/2 lay-up (i.e., three layers aluminum alloy sheet and two layers prepreg) of fiber/metal laminates is shown in Fig. 1. To date, most experience has been obtained on laminate products employing 0.012-in. gauge aluminum sheet; however, 0.0085- and 0.016-in. sheet gauges are also available for use. The first-generation ARALL laminates employ aramid fibers in a uniaxial configuration, while the second-generation GLARE laminates employ glass fibers which may be either in a uniaxial or orthogonal cross-ply arrangement.

Based on our experience with ARALL 3 laminate MIL-HDBK-5 design allowable program[19] and literature search, we found that the bearing strength depends on some relevant parameters. These include: *material parameters* — fiber type and form (unidirectional or biaxial), resin type, fiber orientation, laminate stacking sequence, fiber volume fraction, and fiber surface treatment; *fastener parameters* — fastener type (screw, bolt, or rivet), fastener size, clamping force, washer size, and hole size and tolerance; and *design parameters* — joint type (single lap or single cover butt), laminate thickness and tolerance, geometry (pitch, edge distance, width, hole pattern), load direction, loading rate, static or dynamic load, and failure mode as influenced by specimen geometry and test procedure. This test evaluation program will focus on the study of some of the key factors that influence the bearing

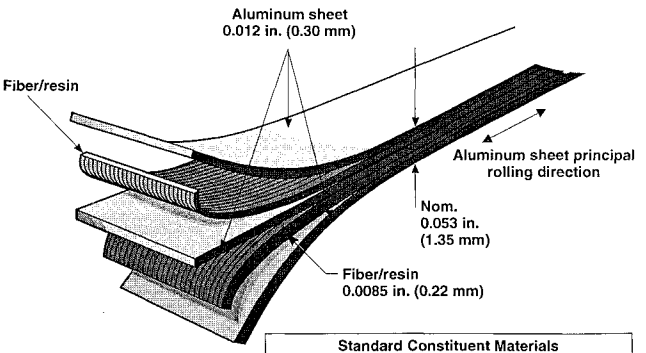

Standard Constituent Materials	
Aluminum sheet alloy	2024 or 7475
Fiber	Aramid or glass
Prepreg	Unidirectional or cross-ply

Fig. 1 Fiber/metal structural laminates (typical 3/2 lay-up shown).

Received Jan. 6, 1993; revision received March 23, 1993; accepted for publication July 2, 1993.

*Staff Engineer, Product Design and Mechanics Division; currently at Owens-Corning Science and Technology Center, Granville, OH 43023.

†Graduate Student, Faculty of Aerospace Engineering.

Table 1 Standardized first-generation laminate product forms

Product variant	Description
ARALL 1	Alloy: 7475-T6, bonding surfaces anodized and primed Prepreg: 250°F cure epoxy-adhesive with unidirectional aramid fibers Postcure 0.4% permanent stretch
ARALL 2	Alloy: 2024-T3, bonding surfaces anodized and primed Prepreg: 250°F cure epoxy-adhesive with unidirectional aramid fibers
ARALL 3	Alloy: 7475-T76, bonding surfaces anodized and primed Prepreg: 250°F cure epoxy-adhesive with unidirectional aramid fibers Postcure 0.4% permanent stretch
ARALL 4	Alloy 2024-T8, bonding surfaces anodized and primed Prepreg: 350°F cure epoxy-adhesive with unidirectional aramid fibers

Table 2 Standardized second-generation laminate product forms

Product variant	Description
GLARE 1	Alloy: 7475-T76, bonding surfaces anodized and primed Prepreg: 250°F cure epoxy-adhesive with unidirectional glass fibers Postcure 0.5% permanent stretch
GLARE 2	Alloy: 2024-T3, bonding surfaces anodized and primed Prepreg: 250°F cure epoxy-adhesive with unidirectional glass fibers
GLARE 3	Alloy: 2024-T3, bonding surfaces anodized and primed Prepreg: 250°F cure epoxy-adhesive with cross-ply glass fibers 50% fibers in longitudinal aluminum sheet direction 50% fibers in long-transverse aluminum sheet direction
GLARE 4	Alloy 2024-T8, bonding surfaces anodized and primed Prepreg: 250°F cure epoxy-adhesive with cross-ply glass fibers 70% fibers in longitudinal aluminum sheet direction 30% fibers in long-transverse aluminum sheet direction

mechanical behavior and will optimize the relevant parameters affecting the bearing strength in fiber/metal laminates. The purpose of this research is not only to develop a meaningful bearing test procedure but also to help designers optimize the edge distance, laminate width, and pinhole size (or laminate thickness). This will assist designers in developing *full* bearing strength for joints in structures and in preventing the mechanical fasteners from failing in shear, tension, or cleavage modes during their operation.

II. Failure Modes

Recently Wu et al.[20,21] presented the *S*-basis minimum strength properties for ARALL 3 laminates from their MIL-HDBK-5 program. In their design allowable program, a large number of static tests were conducted. In the bearing testing, they found that the bearing ultimate strength was strongly dependent on failure modes that influenced by specimen geometry and test method. Failure mechanisms of ARALL laminates showed metal-like typical failure modes such as those shown in Fig. 2. However, their failure mechanisms are more complex and different due to delamination buckling and depend on many factors as described above. Effects of these parameters in bearing test results have been reported in the literature.[22–28]

A. Net-Section Tension Failure

As with conventional materials, the tensile load required to fail a laminate through a section with holes (net-section) is less than at a section in which there are no holes (gross-section). The stresses at these sections, at failure, are given respectively by

$$\sigma_N = P/(W - D)t \tag{1}$$

$$\sigma_G = P/Wt \tag{2}$$

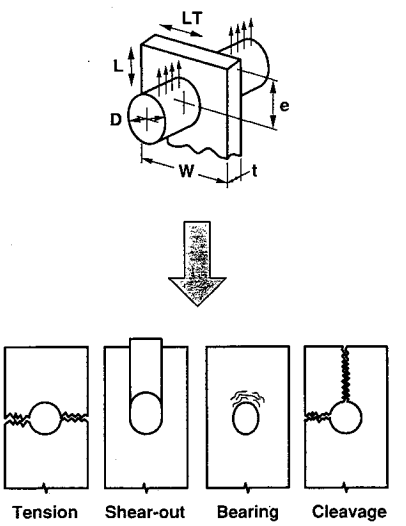

Fig. 2 Typical failure modes of bearing test for ARALL laminates.

where P is the failing load of the laminate, W the laminate width at the gross-section, D the pinhole diameter, and t the laminate thickness. The tensile strength efficiency achieved at these sections, expressed in the form of average net and gross stress concentration, is given by

$$k_N = \sigma_\infty/\sigma_N \tag{3}$$

$$k_G = \sigma_\infty/\sigma_G \tag{4}$$

where σ_∞ is the theoretical ultimate tensile strength of a plain laminate.

B. Shear-Out Failure

The shear strength normally quoted for fiber/metal laminates is the interlaminar shear strength obtained using the short beam shear test. The in-plane shear strength can be measured using the Iosipescu shear test.[29,30] The shear strength, as for conventional isotropic materials, is given as

$$\tau = P/2et \tag{5}$$

where e is the edge distance (parallel to the load) between the hole center and the free edge.

C. Bearing Failure

Bearing of a pin in a hole gives rise to compressive stresses around the loaded half of the circumference of a hole. For practical purposes the bearing strength of hybrid laminates, like that of a conventional material, is usually expressed as the average projected stress acting uniformly over the cross-sectional area of the hole, so that

$$\sigma_b = P/Dt \tag{6}$$

1. Background

In the previous work performed by Wu et al.[20,21] all bearing tests in the MIL-HDBK-5 ARALL 3 laminate design allowable program were conducted in accordance with ASTM E-238[31] test procedure, which is applicable to conventional aluminum alloy products as described in MIL-HDBK-5. Bearing strengths in both the longitudinal L and long-transverse LT directions with the e/D ratios of 1.5 and 2.0 were used in the test program. Here, L is also parallel to aluminum alloy sheet principal rolling direction and LT is perpendicular to the principal rolling direction of aluminum alloy sheet. Four types of lay-up of ARALL 3 laminates (2/1, 3/2, 4/3, and 5/4) were selected. Six tests per test direction per lay-up were performed. Table 3 summarizes the failure modes of these bearing tests in the MIL-HDBK-5 program.

As the width of the specimen decreases, there is a point where the mode of failure changes from bearing to net-section tension, i.e., the specimen fails across the width at the net-section, with cracks originating from the hole boundary. As the edge distance decreases, the bearing failure mode changes to one of shear-out. In this design allowable program, the results show that a total number of 96 bearing tests in the L direction having $e/D = 1.5$ failed in either shear-out or cleavage mode. This indicates that the full bearing strength was not totally achieved when the edge distance ratio equals 1.5 in the longitudinal test specimen. The remaining 288 tests failed in the bearing mode. However, a delamination buckling bearing failure commonly occurred around the pinhole for ARALL laminates. The absence of lateral constraint in this test setup allows this type of failure which has been analyzed and discussed extensively in Ref. 32. Previous work[27,28,32] has also demonstrated that lateral constraint substantially enhances the bearing strength performance of laminates. Contrarily, aluminum alloy sheet usually showed more uniform deformation of bearing failure around the pinhole area. This suggests that an out-of-plane buckling failure of ARALL laminates has occurred during the test.

2. Hypothesis

The anisotropic nature of fibers may also induce a high magnitude of stress concentration around the pinhole. Several hypotheses can be drawn from various failure mode observations:

1) High stress concentration magnitudes occur around the pinhole due to the nature of anisotropy of the hybrid laminates.

2) Full bearing strength is not developed with current parameters of e/D, W/D, and D/t ratios (geometry effect).

3) Delamination buckling is a typical bearing failure mode if lateral constraint is not provided.

4) Premature bearing failure happened because of lacking lateral constraint during the testing.

The present experimental program was directed toward addressing these concerns and hypotheses.

III. Experimental Program

A. Testing Variables

The bearing strength and the failure modes of fiber-reinforced aluminum laminates depend on four geometric variables: 1) the edge distance, 2) the width, 3) the pinhole diameter, and 4) the laminate thickness. Another important variable is the testing procedure that is used with or without lateral constraint. A test matrix of bearing strength characterization for ARALL and GLARE laminates on the e/D, W/D, and D/t effects is described in Table 4.[33] Two test procedures, the pin-type bearing[31] and the bolt-type bearing[34] test methods were investigated in this program. Figure 3 demonstrates the details of these two types of bearing test methods. The pin-type bearing test procedure is characterized by the lack of lateral constraint in contrast to the bolt-type bearing test procedure which can provide lateral constraint. The bearing ultimate strength obtained from the pin-type testing procedure (ASTM E-238) is calculated by dividing the maximum load carried by the specimen by the bearing area, whereas the bearing ultimate strength obtained from the bolt-type testing procedure (ASTM D-953) is defined by the maximum load occurring before a 4% total deflection of the original pinhole, divided by the bearing area. The typical load deflection curves using the pin-type and bolt-type bearing test procedures are shown in Fig. 4.

B. Statistical Design

Two randomizations were involved in carrying out these statistically designed experiments.[33] The first was the random

Table 3 Summary of ARALL 3 laminate bearing failure modes distribution

Edge distance ratio	$e/D = 1.5$						$e/D = 2.0$					
Test direction[a]	L			LT			L			LT		
Failure mode[b]	S	B	C	S	B	C	S	B	C	S	B	C
Lay-up												
2/1	24	—	—	—	24	—	—	24	—	—	24	—
3/2	24	—	—	—	24	—	—	24	—	—	24	—
4/3	24	—	—	—	24	—	—	24	—	—	24	—
5/4	—	—	24	—	24	—	—	24	—	—	24	—

[a] L — longitudinal; LT — long-transverse.
[b] S — shear-out mode; B — bearing mode; C — cleavage mode (refer to Fig. 2).

Table 4 Test matrix of bearing strength characterization for fiber/metal laminates

Type of test	Laminates		
	ARALL 2	GLARE 2	GLARE 3
Metal volume fraction, %	67.90	64.29	64.29
Test direction	*L* and *LT*	*L* and *LT*	*L*
e/D (fixed *W/D* = 6)	1.5, 2, 3, 5	1.5, 2, 3, 5	1.5, 2, 3, 5
W/D (fixed *e/D* = 3)	2, 4, 6, 8	2, 4, 6, 8	2, 4, 6, 8
D/t (fixed *e/D* = 3 and *W/D* = 6 with lateral constraint)	—	Three laminate thickness: 2/1 (V_f)Al. = 70.59% 3/2 (V_f)Al. = 64.29% 5/4 (V_f)Al. = 60.00% @ Three hole sizes (4, 6.35, and 8 mm)	—
With lateral constraint (modified ASTM D-953)	No	Yes	Yes
No lateral constraint (ASTM E-238)	Yes	Yes	No

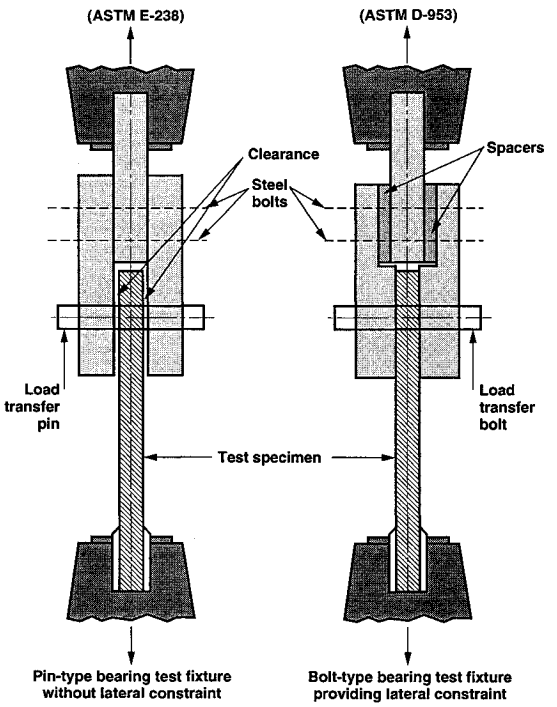

Fig. 3 Schematic representation of pin-type and bolt-type bearing testing procedures.

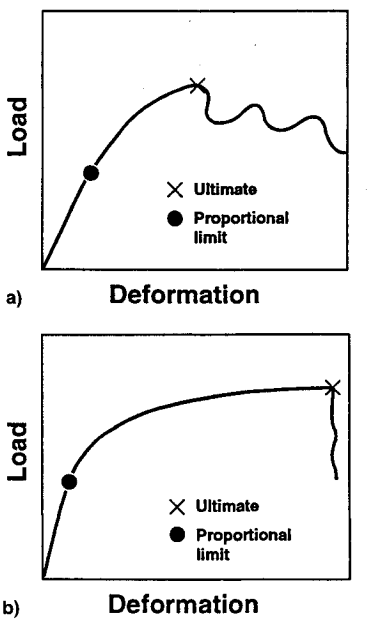

Fig. 4 Typical load-deformation curves using a) pin-type and b) bolt-type bearing test setups.

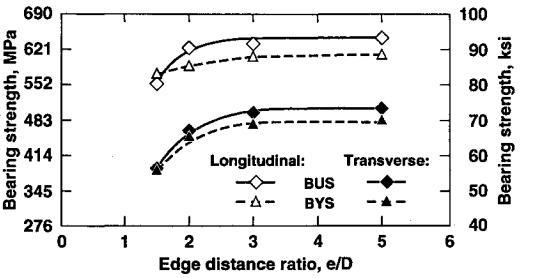

Fig. 5 4/3 ARALL 2 laminate pin-type bearing ultimate and yield strengths variation with *e/D* ratio.

assignment of the treatment variables to the specimens cut from each panel. This was done to guard against systematic variations in the properties of the material with position on the panel. The second randomization involved testing the samples in a random time order. This guarded against a systematic drift in the testing system with time. In this experimental program, the quadruplicate tests were performed in both *L* and *LT* directions using two different test procedures. Data plotted in the following figures represent an average value from four test data.

IV. Results and Discussion

A. Effect of Edge Distance

As the edge distance decreases, the mode of failure changes from bearing to shear-out. Tests varying the *e/D* ratio of 1.5, 2, 3, and 5 were studied on ARALL 2, GLARE 2, and GLARE 3 laminates. Test results are plotted in Figs. 5–7. In these figures, the transition region of bearing strength of ARALL or GLARE laminates had been developed when $e/D \geq 3$. The *e/D* effect is shown to be independent of test method. In the tests, the bolt-type bearing test method provided lateral side restraint to reduce stress concentration around the pin-hole. This caused the stresses to be distributed more uniformly over a larger area than in a pin-type loaded specimen, resulting in a higher bearing strength.

B. Effect of Width

As the width of the specimen decreases, there is a point where the mode of failure changes from bearing to net-section tension. Tests varying the *W/D* ratio of 2, 4, 6, and 8 were investigated on ARALL and GLARE laminates. Test results are presented in Figs. 8–10. It is important to note that the gradual asymptotic behavior of the curves of the ARALL or GLARE laminates has occurred, revealing a strong influence of the width on the bearing failure load. In the figures, the

Table 5 Comparison between longitudinal bearing ultimate strengths (BUS) obtained by bolt-type bearing tests and the rule-of-mixtures for 3/2 GLARE 2 and GLARE 3 laminates[32]

Lay-up (aluminum layer thickness, mm)	Aluminum volume fraction, %	BUS, MPa		
		Experimental	Theory	Difference %
GLARE 2 laminates[a]				
3/2 (0.5)	75.00	767	762	−0.7
4/3 (0.4)	68.09	714	707	−1.0
5/4 (0.4)	66.67	689	696	+1.0
5/4 (0.3)	60.00	639	643	+0.6
3/2 (0.3)	64.29	709	677	−4.5
GLARE 3 laminates[b]				
3/2 (0.3)	64.29	789	726	−8.0
2/1 (0.2)	61.54	810	709	−12.5
2/1 (0.3)	70.59	856	768	−10.3
3/2 (0.2)	54.55	702	663	−5.6
4/3 (0.4)	68.09	778	751	−3.5
4/3 (0.5)	72.73	832	781	−6.1
5/4 (0.4)	66.67	769	742	−3.5

[a] σ_{bus}^{Al} = 959 MPa for 2024-T3 aluminum alloy sheet bearing ultimate strength; σ_{bus}^{p} = 170 MPa for unidirectional cured glass prepreg bearing ultimate strength.
[b] σ_{bus}^{Al} = 959 MPa for 2024-T3 aluminum alloy sheet bearing ultimate strength; σ_{bus}^{p} = 308 MPa for cross-ply cured glass/epoxy prepreg bearing ultimate strength.

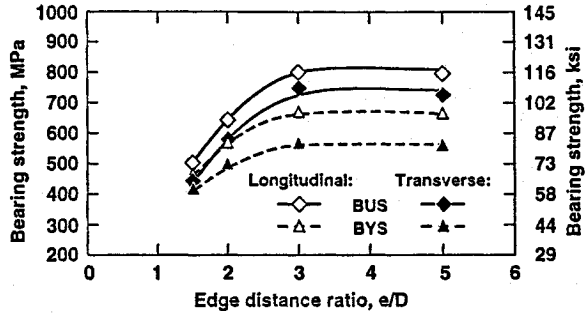

Fig. 6 3/2 GLARE 2 laminate bolt-type bearing ultimate and yield strengths variation with *e/D* ratio.

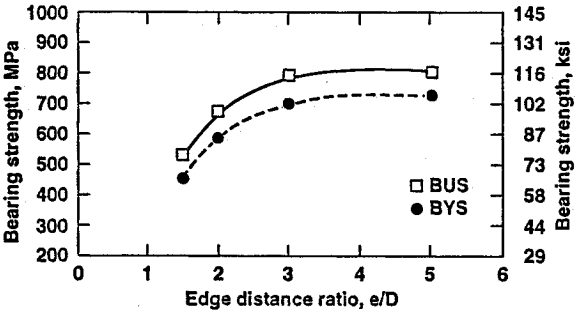

Fig. 7 3/2 GLARE 3 laminate bolt-type longitudinal bearing ultimate and yield strengths variation with *e/D* ratio.

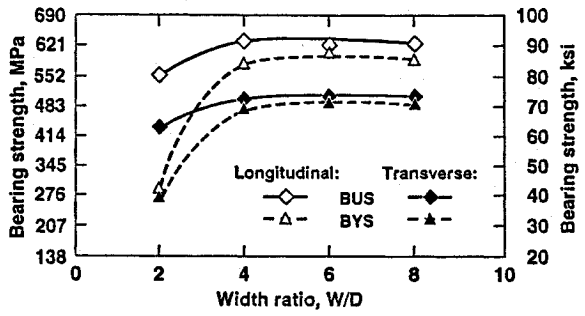

Fig. 8 4/3 ARALL 2 laminate pin-type bearing ultimate and yield strengths variation with *W/D* ratio.

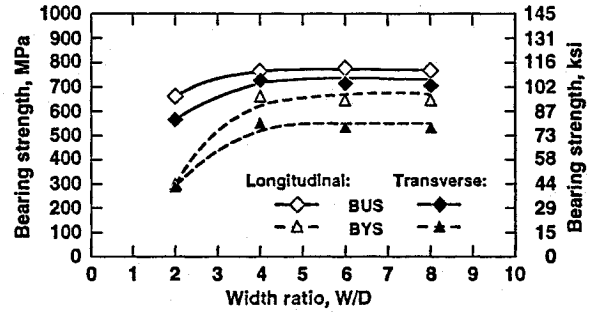

Fig. 9 3/2 GLARE 2 laminate bolt-type bearing ultimate and yield strengths variation with *W/D* ratio.

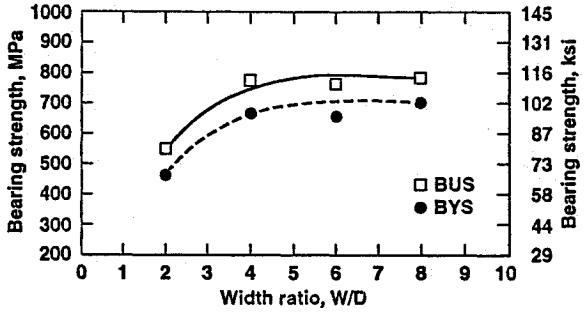

Fig. 10 3/2 GLARE 3 laminate bolt-type longitudinal bearing ultimate and yield strengths variation with *W/D* ratio.

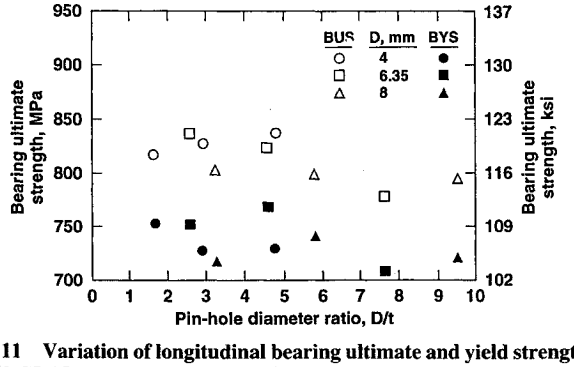

Fig. 11 Variation of longitudinal bearing ultimate and yield strengths of 3/2 GLARE 2 laminates with *D/t* ratio (finger-tight bolt), t = 0.84, 1.38, or 2.47 mm.

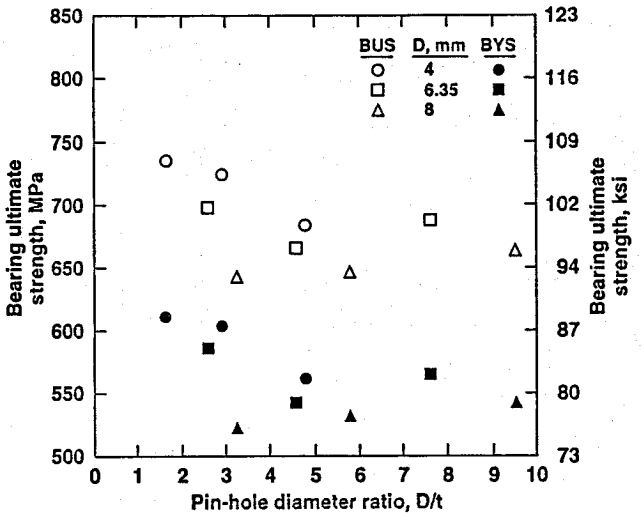

Fig. 12 Variation of long-transverse bearing ultimate and yield strengths of 3/2 GLARE 2 laminates with D/t ratio (finger-tight bolt), t = 0.84, 1.38, or 2.47 mm.

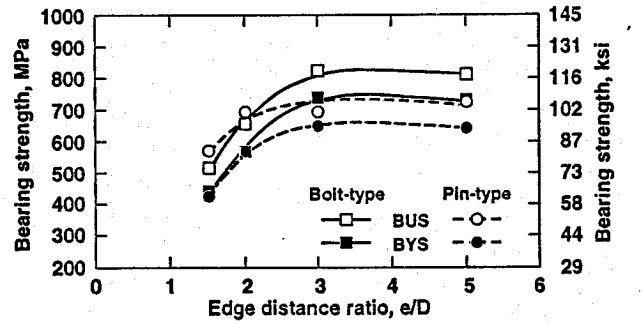

Fig. 13 Comparison of longitudinal bearing ultimate and yield strength of 3/2 GLARE 2 laminates vs e/D ratio using bolt-type and pin-type test fixtures.

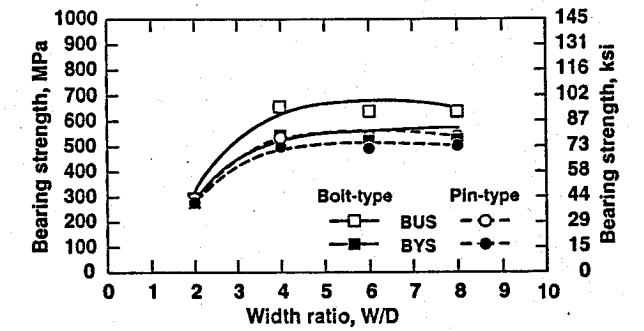

Fig. 14 Comparison of long-transverse bearing ultimate and yield strength of 3/2 GLARE 2 laminates vs W/D ratio using bolt-type and pin-type test fixtures.

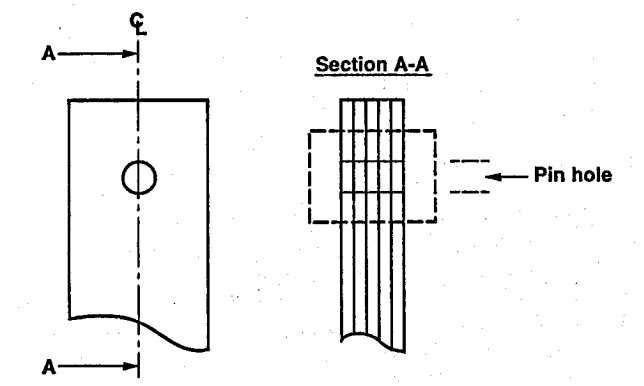

Fig. 15 Cross section through fiber/metal laminate bearing specimen center for failure modes observation.

transition region of bearing strength occurs when $W/D \geq 4$. A D/W value of about 0.25 provides optimum joint structural efficiency which agrees with the Hart-Smith's interpretation of bolted joint data in fibrous materials.[35]

C. Effect of Thickness

Effect of thickness was found if the ratio D/t was examined. In Figs. 11 and 12, it is clear that bearing ultimate strength increases with decreasing D/t ratio for the case of finger-tight bolt-type bearing tests on GLARE 2 laminates. From the current chosen range of holes of 4- to 8-mm diam in these two figures, the effect of the pin diameter on bearing strength in the L direction seems to be more pronounced than in the LT direction. However, effect of the pin diameter on bearing strength in the LT direction shows insignificantly different when $D/t \geq 3$. Although, in reality, when we attempt to avoid the influence of aluminum volume fraction (by considering a single lay-up) the effect is rather small (even <5%). Collings[26] and Godwin and Matthews[22] presented similar results for car-

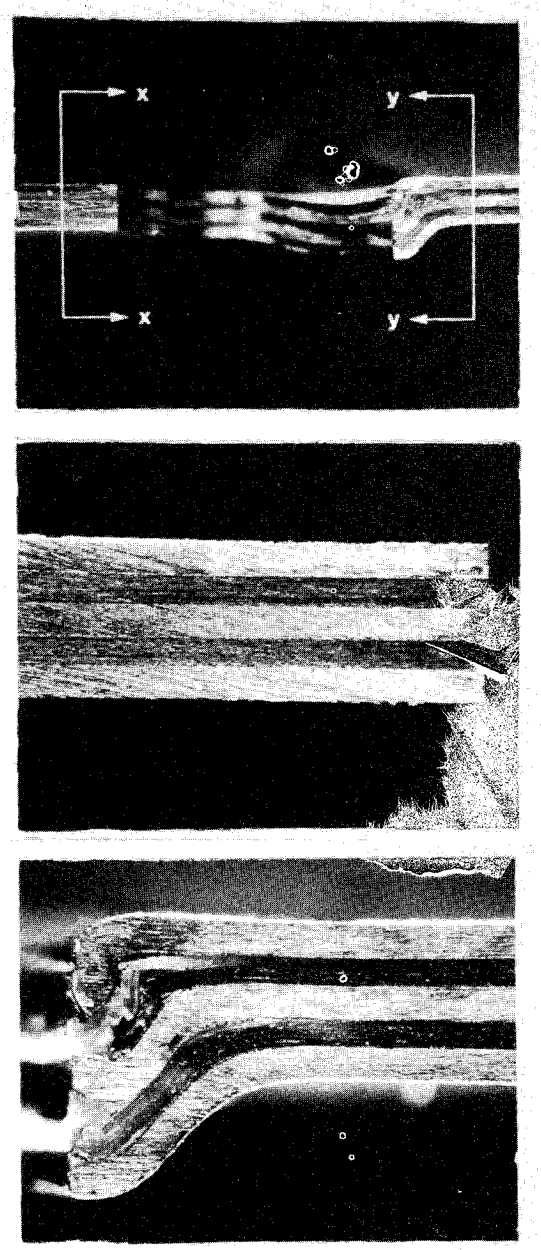

Fig. 16 Delamination buckling of bearing failure of 3/2 GLARE 2 laminates tested in the longitudinal direction with no lateral constraints. ASTM E-238: bearing load = 7478 N, bearing strength = 688 MPa, e/D = 3, and W/D = 8 (D = 8 mm): a) 7X; b) undeformed portion, 25X (view x-x); and c) deformed portion, 25X (view y-y).

bon/epoxy composites and other materials, but Collings showed that for high lateral pressure values, the effects of D/t almost disappear.

D. Effect of Lateral Constraint

Studies by Stockdale and Matthews[27] for glass fiber-reinforced plastics and Eriksson[28] for graphite/epoxy laminates have been shown a significant influence on the effect of lateral constraint in the bearing tests. A finger-tight pressure was applied to the bolt-type bearing test fixture. This type of side restraint bearing loading provided a sufficient lateral constraint on the part of the laminate to control the delamination buckling mode. The ultimate load is therefore expected to increase since the earliest failure modes are suppressed. However, the failure mode of the pin-type bearing specimens showed the damage being localized around the loaded half of the hole. And the delamination buckling was easily observed. Figures 13 and 14 show the comparison in bearing strengths variation with e/D and W/D ratios using these two types of test fixture, respectively. Results show that the bolt-type test method yields at least a 20% increase in bearing strength over that of the pin-type test method when $e/D \geq 3$ and $W/D \geq 4$.

E. Effect of Fiber Orientation

The fiber orientation in the laminate affects both the bearing strength and mechanism of failure. Results show that the bearing strength obtained from the longitudinal test direction which is parallel to metal principal rolling direction is greater than that of the long-transverse test direction which is perpendicular to metal principal rolling direction as shown in the unidirectional ARALL or GLARE laminates (see Fig. 1). This implies that the fibers contribute more to the bearing performance. The GLARE 3 laminates, the cross-ply configuration (50% of fibers in 0-deg orientation and 50% of fibers in 90-deg orientation in each prepreg layer), we only acquired one direction bearing strength which is parallel to metal principal rolling direction.

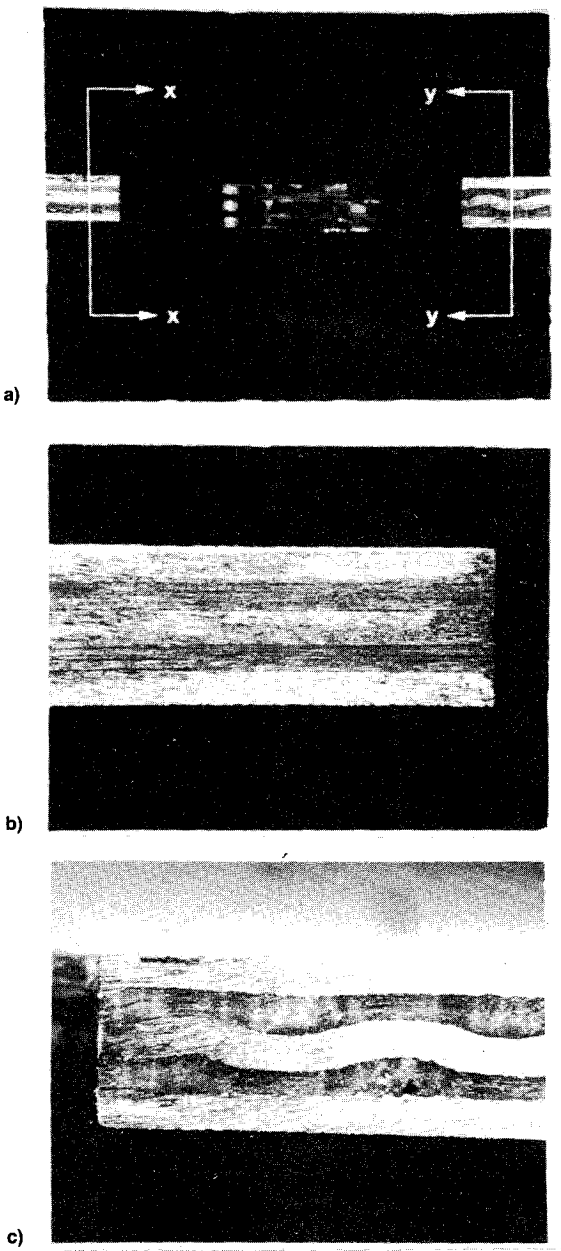

Fig. 17 Delamination buckling free of bearing failure of 3/2 GLARE 2 laminates tested in the longitudinal direction with lateral constraints. ASTM D-953: bearing load = 10,867 N, bearing strength = 977 MPa, e/D = 3, and W/D = 6 (D = 8 mm): a) 7X; b) undeformed portion, 25X (view x-x); and c) deformed portion, 25X (view y-y).

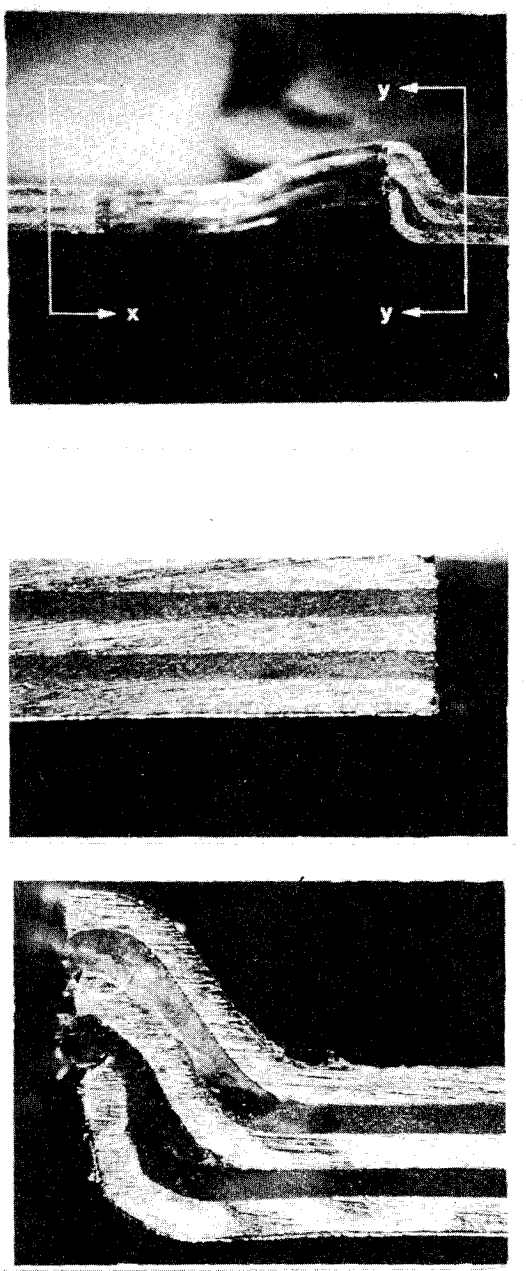

Fig. 18 Delamination buckling of bearing failure of 3/2 GLARE 2 laminates tested in the long-transverse direction with no lateral constraints. ASTM E-238: bearing load = 6137 N, bearing strength = 548 MPa, e/D = 3, and W/D = 6 (D = 8 mm): a) 7X; b) undeformed portion, 25X (view x-x); and c) deformed portion, 25X (view y-y).

F. Bearing Strength Prediction

A rule-of-mixtures approach can be applied to the prediction of fiber/metal laminate bolt-type bearing ultimate strength. This has been proven for an edge distance ratio $e/D = 2$ in Ref. 32. In the rule-of-mixtures, we assume that bearing failure occurs in the laminate when the individual layers (prepreg and aluminum) collapse simultaneously. This is because the separate layer stiffness will not play any significant role. This simple analysis is based on the aluminum volume fraction of the laminate:

$$\sigma_{lam} = V_{al} \times \sigma_{al} + (1 - V_{al}) \times \sigma_p \qquad (7)$$

where σ_{lam} is the laminate bearing ultimate strength, σ_{al} the aluminum alloy bearing ultimate strength, σ_p the cured fiber/epoxy prepreg bearing ultimate strength, and V_{al} the aluminum alloy volume fraction.

A comparison between the longitudinal bearing ultimate strengths obtained from the bolt-type bearing test procedure and the theoretical values predicted by the rule-of-mixtures for GLARE laminates are presented in Table 5. The results demonstrate that a good prediction in bearing ultimate strength of GLARE 2 laminates was achieved. The relatively lower calculated stresses for GLARE 3 laminates are perhaps due to the beneficial contribution of cross-ply fibers in the overall laminate sandwich.

G. Bearing Failure Mode Observations

Observations of failure modes of the tested GLARE 2 laminate bearing specimens in both the L and LT directions obtained from pin-type (unconstrained) and bolt-type (constrained) testing procedures were examined using optical microscopy. Photomicrographs were taken from above and below the pinhole along section A-A as illustrated in Fig. 15. Figures 16 and 17 show bearing failure patterns of GLARE 2 laminates in the L direction for both testing procedures. Bearing failure patterns of GLARE 2 laminates in the LT direction for both testing procedures are shown in Figs. 18

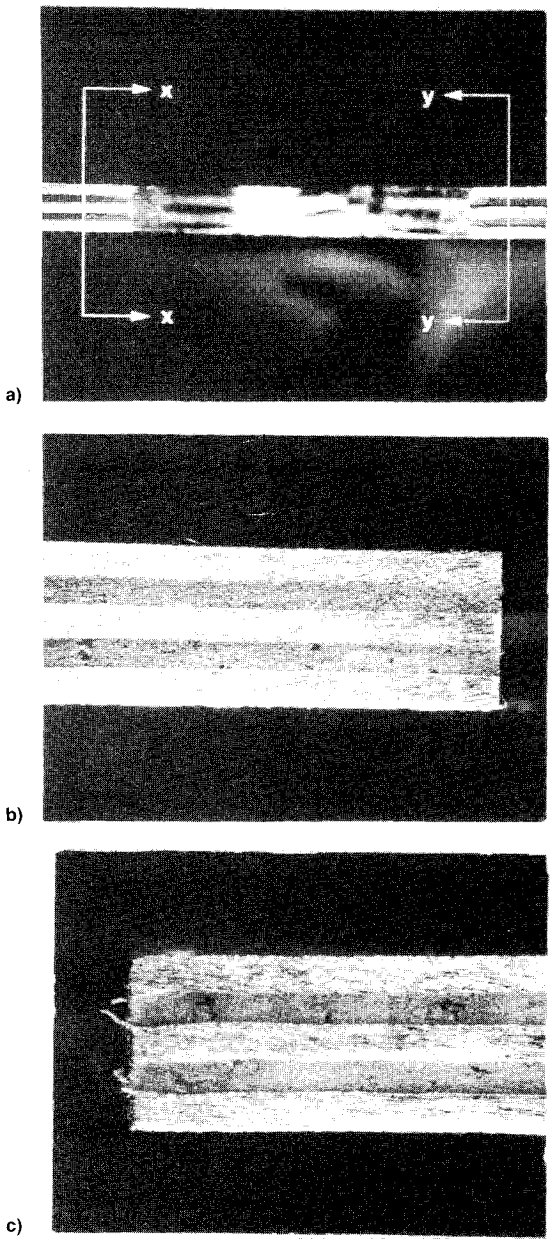

Fig. 19 Delamination buckling free of bearing failure of 3/2 GLARE 2 laminates tested in the long-transverse direction with lateral constraints. ASTM D-953: bearing load = 10,742 N, bearing strength = 959 MPa, $e/D = 3$, and $W/D = 6$ ($D = 8$ mm): a) 7X; b) undeformed portion, 25X (view x-x); and c) deformed portion, 25X (view y-y).

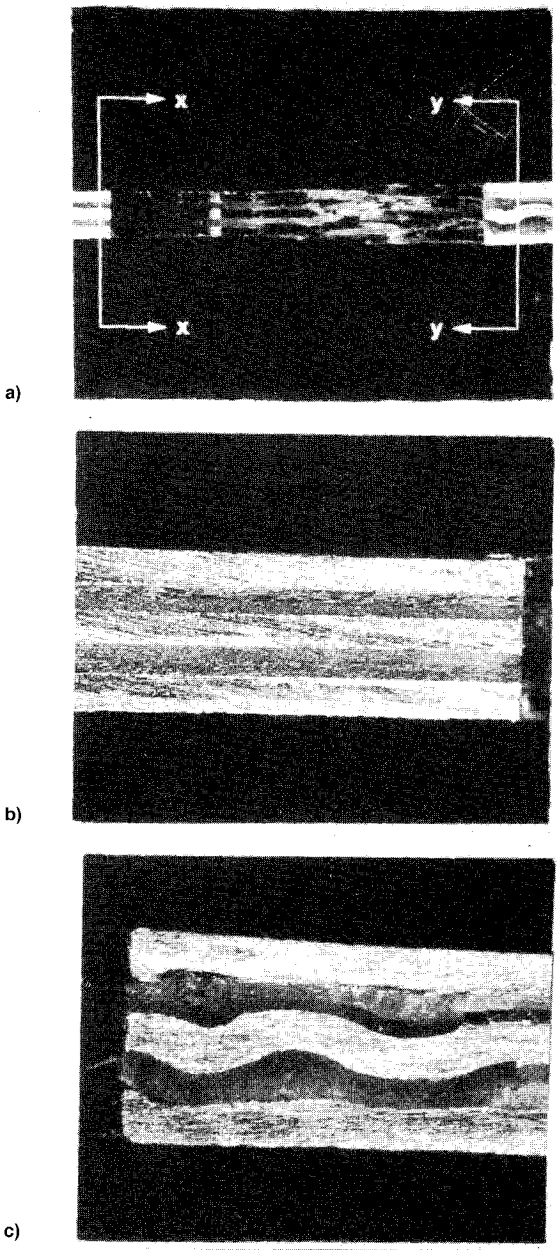

Fig. 20 Delamination buckling free of bearing failure of 3/2 GLARE 3 laminates tested in the longitudinal direction with lateral constraints. ASTM D-953: bearing load = 11,422 N, bearing strength = 1017 MPa, $e/D = 3$, and $W/D = 6$ ($D = 8$ mm): a) 7X; b) undeformed portion, 25X (view x-x); and c) deformed portion, 25X (view y-y).

and 19. The figures indicate that a delamination buckling bearing failure has been observed in the testing procedure which has no side constraint (ASTM E-238); however, no visual evidence of macrodelamination buckling bearing failure was found using testing procedure of ASTM D-953 (with lateral constraint). Because no delamination buckling occurs in the latter testing procedure, a bearing ultimate strength increase over pin load specimen values is to be expected. Another interesting finding is that the wavy deformation (in-phase mode of buckling) found in the center layers of aluminum alloy of the laminate in the L direction is due to the central aluminum alloy layer being compressed by both sides of fiber prepregs. A similar phenomena is also seen in GLARE 3 laminates as shown in Fig. 20. However, this aluminum alloy wavy deformation is not found in the LT oriented bearing specimens. This wavy deformation of center layer of aluminum alloy sheet inspires a great interest of future research for further understanding the bearing failure analysis.

H. Joint Structural Efficiency

Joint structural efficiency is defined as a computed ratio of joint strength to laminate tensile strength. Diagrams of joint efficiency are used for structural fastened joint design for aerospace applications. Hart-Smith[35] has investigated the relationship between strengths of bolted joints in ductile, fibrous composites, and brittle materials. Based on the bearing strength data obtained from the effect of pinhole diameter-to-width ratio, the joint structural efficiency diagrams of GLARE laminates in both the L and LT directions have been established, as shown in Figs. 21 and 22. These curves of GLARE 2 laminates were derived purely on the basis of bearing test results. There are bearing failures at the left region of the picture (when $W/D \geq 4$, where the bearing specimen width is large in comparison with the hole diameter. As the pinhole is moved closer to the side edge of the specimen (or the specimen is narrowed), there is a change in failure mode to tension-through-the-hole (when $W/D \leq 2$).

In Figs. 21 and 22, the peak strength occurs either at a geometry associated with the tension failure mode or at an abrupt transition between bearing and tension failures, and that, in either case, peak strength is associated with a definite W/D value, which is projected to value of 4 for long-transverse orientation GLARE 2 laminates and a value of 2 for longitudinal orientation GLARE 2 laminates in the bolt-type testing procedure. Any effort to impose on a bolted composite joint design an arbitrary requirement of failure by bearing only (by using a sufficiently large value of W/D) to ensure a less catastrophic failure mode must necessarily be associated with a significant reduction in joint strength and, hence, in structural efficiency. In addition, results show that joint structural efficiencies in both the L and LT directions have a compatible trend as compared with fibrous composites and ductile materials,[35] respectively.

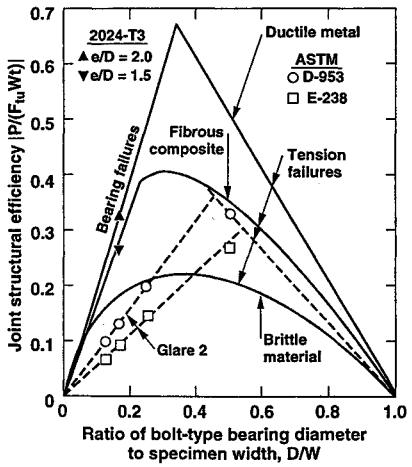

Fig. 21 Relation between strengths of bolted joints in ductile, fibrous composites, and brittle materials (Ref. 35, Hart-Smith, 1978) as compared with longitudinal 3/2 GLARE 2 laminates.

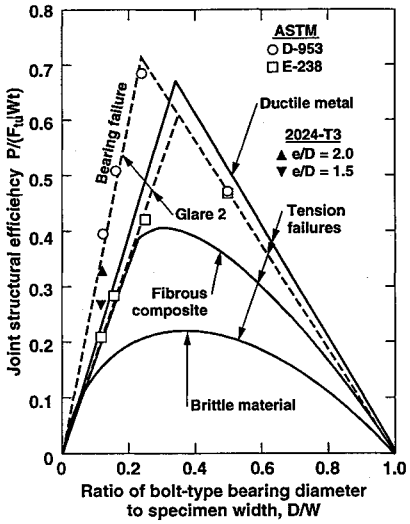

Fig. 22 Relation between strengths of bolted joints in ductile, fibrous composites, and brittle materials (Ref. 35, Hart-Smith, 1978) as compared with long-transverse 3/2 GLARE 2 laminates.

V. Conclusions

From this study, several conclusions can be drawn as follows:

1) Fiber/metal laminate bearing strength is shown to depend on failure mode as influenced by specimen geometry and test method.

2) A bearing test fixture with lateral constraint (bolt-type) produces a more representative structural failure mode than does the unconstrained pin-type test.

3) A bolt-type test fixture (modified ASTM D-953) gives a bearing strength at least 20% higher than that given by a pin-type test fixture (ASTM E-238) when the full bearing strength is being developed.

4) A minimum edge distance ratio e/D of 3 and width ratio W/D of 4 should be used to develop the full bearing strength for fiber/metal laminates.

5) A D/W value of about 0.25 for long-transverse orientation specimen or 0.45 for longitudinal orientation specimen provides optimum joint structural efficiency when bolt-type bearing testing procedure is employed. The joint structural efficiency of long-transverse orientation GLARE 2 laminates has shown comparable with those aluminum alloy sheets.

6) A rule-of-mixtures approach can be applied to prediction of bolt-type bearing ultimate strength in fiber/metal laminates.

VI. Recommendations

The detailed mechanism of wavy deformation of the center layer of aluminum alloy sheet in the longitudinal bearing test specimen should be further studied. Failure mechanism can be correlated to its monotonical bearing behavior which is exhibited in the load vs displacement curve. Bearing properties on both cured fiber/epoxy prepregs and pure aluminum alloy sheets should be determined based on the geometry effect for the support of using the rule-of-mixtures prediction.

Acknowledgments

The authors wish to thank M. Hakker of Delft University for performing the experimental work and J. C. Vilsack of the Alloy Technology Division on providing photomicrographs of failure mode study. Finally, technical discussions from R. J. Bucci and a number of statistical analysis and plots generated by Ling L. Wu are also gratefully acknowledged.

References

[1]Marrissen, R., and Vogelesang, L. B., "Development of a New Hybrid Material: ARALL," International SAMPE Conf., Cannes, France, 1981.

[2]Vogelesang, L. B., Marissen, R., and Schijve, J., "A New Fatigue Resistant Material: Aramid Reinforced Aluminum Laminate (ARALL)," 11th ICAF Symposium, Noordwijkerhout, The Netherlands, 1981.

[3]Gunnink, J. W., Vogelesang, L. B., and Schijve, J., "Application of a New Hybrid Material (ARALL) in Aircraft Structures," *Proceedings of the 13th Congress International Council Aerospace Science* (Seattle, WA), 1982, pp. 990–1000 (ICAS-82-2.6.1).

[4]Vogelesang, L. B., and Gunnink, J. W., "ARALL, A Material for the Next Generation of Aircraft, a State-of-the-Art," Dept. of Aerospace Engineering, Delft Univ. of Technology, Rept. LR-400, The Netherlands, 1983.

[5]Gunnink, J. W., Verbruggen, M. L. C. E., and Vogelesang, L. B., "ARALL, a Lightweight Structural Material for Impact and Fatigue Sensitive Structures," *Vertica*, Vol. 10, No. 2, 1986, p. 241.

[6]Vogelesang, L. B., and Gunnink, J. W., "ARALL: A New Material Challenge for the Next Generation of Aircraft," *Materials and Design*, Vol. 7, No. 2, 1986.

[7]Bucci, R. J., Mueller, L. N., Schultz, R. W., and Prohaska, J. L., "ARALL Laminates—Results from a Cooperative Test Program," Materials—Pathway to the Future, *Proceedings of the 32nd International SAMPE Symposium and Exhibition* (Anaheim, CA), 1987, pp. 902–916.

[8]*Proceedings of ARALL Laminates Technical Conference*, ed. by Alcoa Laboratories, Alcoa Center, Champion, PA, 1987.

[9]Bucci, R. J., Mueller, L. N., Vogelesang, L. B., and Gunnink, J. W., "ARALL Laminates," *Aluminum Alloys—Contemporary Research and Applications, Treatise on Materials Science and Technology*, Vol. 31, Academic Press, San Diego, CA, 1989, pp. 295–322.

[10]Gunnink, J. W., and Vogelesang, L. B., "Aerospace ARALL: The Advancement in Aircraft Materials," Advanced Materials—The Challenge for the Next Decade, *Proceedings of the 35th International SAMPE Symposium and Exhibition* (Anaheim, CA), 1990, pp. 1708–1721.

[11]Gunnink, J. W., and Vogelesang, L. B., "Aerospace ARALL: A Challenge for the Aircraft Designer," How Concept Becomes Reality, *Proceedings of the 36th International SAMPE Symposium and Exhibition*" (San Diego, CA), 1991, pp. 1509–1522.

[12]Gregory, M. A., and Roebroeks, G. H. J. J., "Fiber/Metal Laminates: A Solution to Weight, Strength, and Fatigue Problems," 30th Annual Conf. of Metallurgists, Metallurgical Society of CIM, Ottawa, Canada, 1991.

[13]Van Veggel, L. H., "The Evolution from Bonded F27 Aircraft Structures," 42nd Annual General Meeting of the Aeronautical Society of India, Calcutta, India, 1990.

[14]Leodolter, W., and Pettit, R. G., "Production Implementation of ARALL Laminate Structures," Specialist Conf. on ARALL Laminates, Delft Univ. of Technology, Douglas Paper 8164, The Netherlands, 1988.

[15]Pettit, R. G., "ARALL Applications of Large Transport Aircraft," AEROMAT '91, Long Beach, CA, 1991.

[16]Wu, H. F., "Temperature Dependence of the Tensile Properties of ARALL-4 Laminates," *Journal of Materials Science*, Vol. 25, No. 2A, 1990, pp. 1120–1127.

[17]Wu, H. F., "Effect of Temperature and Strain Rate on the Tensile Properties of ARALL-1 Laminates," *Journal of Materials Science*, Vol. 26, No. 14, 1991, pp. 3721–3729.

[18]Wu, H. F., "Temperature Dependence of the Tensile Behavior of Aramid/Aluminum Laminates," *Journal of Materials Science*, Vol. 28, 1993, pp. 19–34.

[19]"Metallic Materials and Elements for Aerospace Vehicles Structures," *Military Handbook (MIL-HDBK-5F)*, Vols. 1 and 2, U.S. Dept. of Defense, Washington, DC, 1990.

[20]Wu, H. F., Bucci, R. J., Wygonik, R. H., and Rice, R. C., "Generation of MIL-HDBK-5 Design Allowables for ARALL Laminates," *AEROMAT '91*, Long Beach, CA, May 1991; also *ICCM/8*, Honolulu, HI, July 1991.

[21]Wu, H. F., Bucci, R. J., Wygonik, R. H., and Rice, R. C., "Generation of MIL-HDBK-5 Design Allowables for Aramid/Aluminum Laminates," *Journal of Aircraft*, Vol. 30, No. 2, 1993, pp. 275–282.

[22]Godwin, E. W., and Matthews, F. L., "A Review of the Strength of Joints in Fiber-Reinforced Plastics," *Composites*, 1980, pp. 155–160.

[23]Collings, T. A., "Experimentally Determined Strength of Mechanically Fastened Joints," *Joining Fiber-Reinforced Plastics*, Elsevier Applied Science, England, UK, 1987.

[24]Matthews, F. L., "Theoretical Stress Analysis of Mechanically Fastened Joints," *Joining Fiber-Reinforced Plastics*, Elsevier, London, 1987.

[25]Kretsis, G., and Matthews, F. L., "The Strength of Bolted Joints in Glass Fibre/Epoxy Laminates," *Composites*, Vol. 16, April 1985, pp. 92–102.

[26]Collings, T. A., "On the Bearing Strength of CFRP Laminates," *Composites*, July 1982, pp. 241–252.

[27]Stockdale, J. H., and Matthews, F. L., "The Effect of Clamping Pressure on Bolt Bearing Loads in Glass Fibre-Reinforced Plastics," *Composites*, Jan. 1976, pp. 34–38.

[28]Eriksson, I., "On the Bearing Strength of Bolted Graphite/Epoxy Laminates," *Journal of Composite Materials*, Vol. 24, Dec. 1990, pp. 1246–1269.

[29]Adams, D. F., "The Iosipescu Shear Test Method as Used for Testing Polymers and Composite Materials," *Polymer Composites*, Vol. 11, No. 5, 1990, pp. 286–290.

[30]Broughton, W. R., Kumosa, M., and Hull, D., "Analysis of the Iosipescu Shear Test as Applied to Unidirectional Carbon-Fibre Reinforced Composites," *Composites Science and Technology*, Vol. 38, No. 4, 1990, pp. 299–325.

[31]"Standard Test Method for Pin-Type Bearing Test of Metallic Materials," American Society for Testing and Materials E-238, 1984.

[32]Slagter, W. J., "On the Bearing Strength of Fiber Metal Laminates," *Journal of Composite Materials*, Vol. 26, No. 17, 1992, pp. 2542–2566.

[33]Wu, H. F., "Parametric Studies of Bearing Strength for Fiber/Metal Laminates," Structural Laminates Co., SLC Rept. SL-019-C (Project Plan), New Kensington, PA, Oct. 1991.

[34]"Standard Test Method for Bearing Strength of Plastic Properties," American Society for Testing and Materials D-953, 1987.

[35]Hart-Smith, L. J., "Mechanically-Fastened Joints for Advanced Composites—Phenomenological Considerations and Simple Analysis," Douglas Aircraft Co. Paper DP-6748A, Long Beach, CA, Nov. 1978; also *Fibrous Composites in Structural Design*, edited by E. M. Lenoe, D. W. Oplinger, and J. J. Burke, Plenum Press, NY, 1980, pp. 543–574.